Research paper

New pillared dioxomolybdenum(VI) complexes with ONS donor ligands and 4,4′-azopyridine spacer: 3D metal-organic supramolecular architectures and DFT calculations

Debanjana Biswal, Nikhil Ranjan Pramanik, Syamal Chakrabarti, Michael G.B. Drew

PII: S0020-1693(16)30360-7
DOI: http://dx.doi.org/10.1016/j.ica.2016.07.004
Reference: ICA 17139

To appear in: *Inorganica Chimica Acta*

Received Date: 25 March 2016
Revised Date: 13 June 2016
Accepted Date: 1 July 2016

Please cite this article as: D. Biswal, N.R. Pramanik, S. Chakrabarti, M.G.B. Drew, New pillared dioxomolybdenum(VI) complexes with ONS donor ligands and 4,4′-azopyridine spacer: 3D metal-organic supramolecular architectures and DFT calculations, *Inorganica Chimica Acta* (2016), doi: http://dx.doi.org/10.1016/j.ica.2016.07.004

New pillared dioxomolybdenum(VI) complexes with ONS donor ligands and 4,4′-azopyridine spacer: 3D metal-organic supramolecular architectures and DFT calculations

Debanjana Biswal[a], Nikhil Ranjan Pramanik[*b], Syamal Chakrabarti[*a], Michael G.B Drew[c]

[a]*Department of Chemistry, University College of Science, 92, Acharya Prafulla Chandra Road, Kolkata:700009, West Bengal, India.*

[b]*Department of Chemistry, Bidhannagar College, EB-2,Sector-1, Salt Lake, Kolkata: 700064, India.*

[c]*Department of Chemistry, The University of Reading, Whiteknights, Reading RG66AD, UK.*

ABSTRACT

Two new pillared binuclear dioxomolybdenum(VI) complexes $[(MoO_2L^1)_2(4,4'\text{-azpy})]$ (**1**) and $[(MoO_2L^2)_2(4,4'\text{-azpy})]$ (**2**) have been synthesized by the reaction of $MoO_2(acac)_2$ with Schiff base ligands (H_2L^1 and H_2L^2) derived from 2-hydroxyacetophenone and S-benzyl/S-methyl dithiocarbazates respectively and 4,4′-azopyridine as a spacer. Crystal and molecular structures of the investigated binuclear complexes **1** and **2** were determined by single crystal X-ray diffraction. The two complexes have similar centrosymmetric dimeric structures in which each molybdenum atom occupies distorted octahedral six-coordinate environments being bonded to a dianionic tridentate ONS donor ligand via phenolate oxygen, imine nitrogen and thioenolate structure as well as two terminal oxygen atoms and a nitrogen atom of the bridging 4,4'-azpy ligand. Complexes **1** and **2** give rise to 3D metal-organic supramolecular frameworks having rectangular cavities formed via hydrogen bonding and π-π stacking interactions. The complexes

were further characterized by elemental analysis, spectroscopic methods (IR, ^{1}H NMR and UV-Vis), electrochemical study and thermogravimetric analysis. DFT calculations were used to study the electronic properties of the complexes.

Keywords: Dioxomolybdenum(VI), Schiff base ligand, 4,4′-azopyridine, Crystal structure, Supramolecular interactions, DFT calculations

---

*Corresponding authors. Tel: +91- 033-2350-8386; fax: +91-033-2351-9755
Tel: +91- 033-2337-4389; fax: +91-033-2337-4782

E-mail address: schakrabarti2014@gmail.com

nr_pramanik@yahoo.co.in

1. Introduction

The molybdenum complexes of S-benzyl and S-methyl dithiocarbazate Schiff base ligands derived from *ortho*-hydroxyl aldehydes and ketones have been widely studied [1-5]. Interest in the metal complexes of these ligands is stimulated by their interesting physicochemical properties and significant biological activities [6,7]. Schiff base ligands are valued as important sources of biologically active components. Moreover, complexes containing pyridine ring moieties are of great interest due to their extended applicability in biology and pharmacology as antimicrobial, antitubercular, antitumor and analgesic agents [8]. Metal-organic supramolecular frameworks have drawn much attention in recent years not only due to their intriguing structural diversity [9] but also to their wide range of prospective applications in host-guest chemistry [10], catalysis [11], ion-exchange [12], gas-adsorption [13] etc. Molecular self-assembly based on crystal engineering has proved to be efficient for the formation of these architectures. The design and synthesis of bridging ligands [pyrazine, 4,4′-bipyridine, 1,2-bis(4-pyridyl)ethane etc.] containing suitable coordination sites connected by spacers with particular orientations are

especially important for the construction of desirable frameworks. Supramolecular frameworks are constructed mostly via hydrogen bonding and π···π contacts. The hydrogen bond is the most familiar organizing force in supramolecular assemblies due to its moderately directional intermolecular interaction that may control short-range packing [14]. Formation of the inner cavities mostly surrounded by organic components is interesting since the shape, size and function of the cavity become designable. The cavities of the framework are usually occupied by solvent molecules because the crystals have a general tendency to maximize their packing density.

Although molybdenum complexes are of great importance, few articles portray molybdenum complexes as supramolecular architectures [15,16]. The 4,4′-azpy ligand is well-suited for the construction of supramolecular assemblies based on aromatic interactions because of its molecular planarity provided by the π-conjugated system and π orbitals. To realize the pivotal role of non-covalent interactions in supramolecular aggregates of 4,4′-azpy ligand, we describe herein the synthesis, spectroscopic characterization, thermal analyses and electrochemical behavior of two new supramolecular binuclear dioxomolybdenum(VI) complexes $[(MoO_2L^1)_2(4,4'\text{-azpy})]$ (**1**) and $[(MoO_2L^2)_2(4,4'\text{-azpy})]$ (**2**) with primary ONS donor Schiff base ligands together with 4,4′-azpy as the spacer. We also report the crystal structures and structural design of complexes **1** and **2** which exhibit 3D metal-organic supramolecular pillared framework. Single-crystal X-ray analysis gives information about topology and packing of the molecules in the solid state. In these complexes hydrogen bonding plays an important role in the construction of the supramolecular network. Aside from hydrogen bonds, the π···π interaction is another useful organizing force in supramolecular assemblies [17]. Intermolecular interactions have been investigated not only in the context of different crystal packing [18] but also

considering their role in supramolecular architecture formation. In the complexes, the cavities formed by the interaction of the molecules are capable of hosting guest solvent molecules. Calculations regarding structure and energy of the compounds were carried out using DFT.

2. Experimental

2.1. Materials

Reagent grade solvents were dried and distilled prior to use. 4,4′-azobis-(pyridine) (4,4′-azpy) was prepared as an orange solid by the procedure reported previously [19]. All other chemicals used for preparative work were of reagent grade, available commercially and used without further purification.

2.2. Synthesis

2.2.1. Synthesis of the ligands

The Schiff base ligands H_2L^1 and H_2L^2 were prepared by condensing 2-hydroxyacetophenone and S-benzyl/ S-methyl dithiocarbazate in ethanol by methods reported previously [1] (Scheme 1). The ligands were satisfactorily characterized by elemental analyses, IR and ^{1}H NMR.

*S-benzyl-β-N-(2-hydroxyphenylethylidine)dithiocarbazate (**H_2L^1**).* Yield ~ 80%, Anal. Calc. for $C_{16}H_{16}S_2N_2O$ (%): C, 60.76; H, 5.06; N, 8.86, Found: C, 60.22; H, 4.80; N, 8.79, IR (KBr Pellet), cm^{-1}: $\nu_{(O-H)}$ 3435(m), $\nu_{(N-H)}$ 3170(m), $\nu_{(C=N)}$ 1600(s), $\nu_{(C=S)}$ 1311(s); ^{1}H NMR($CDCl_3$): (-S-CH_2-) 4.41 s (2H), (aromatic protons) 6.90-7.45 m (9H), (H_3C-C=N) 2.47 s (3H), (-NH-) 11.25 s (1H), (aromatic -OH) 11.26 s (1H).

*S-methyl-β-N-(2-hydroxyphenylethylidine)dithiocarbazate (**H_2L^2**).* Yield ~ 75%, Anal. Calc. for $C_{10}H_{12}S_2N_2O$ (%): C, 50.00; H, 5.00; N, 11.66, Found: C, 49.71; H, 4.89; N, 11.43, IR (KBr

Pellet), cm^{-1}: $\nu_{(O-H)}$ 3432(m), $\nu_{(N-H)}$ 3172(m), $\nu_{(C=N)}$ 1600(s), $\nu_{(C=S)}$ 1342(s); ^1H NMR($CDCl_3$): (-S-CH_3) 2.53 s (3H), (aromatic protons) 6.87-7.60 m (4H), (H_3C-C=N) 2.46 s (3H), (-NH-) 11.42 s (1H), (aromatic -OH) 12.68 s (1H).

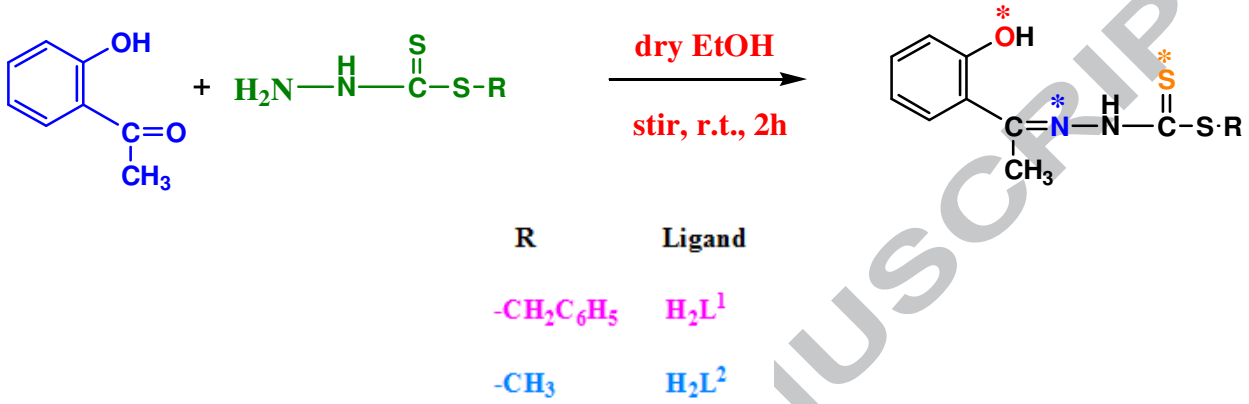

R	Ligand
$-CH_2C_6H_5$	H_2L^1
$-CH_3$	H_2L^2

Scheme 1 Reaction diagram for isolation of the ligands

2.2.2. Synthesis of the complexes

The two mononuclear complexes MoO_2L^1 and MoO_2L^2 were prepared by refluxing $MoO_2(acac)_2$ and the respective ligands in a 1:1 molar ratio in chloroform for 2h. The complexes were satisfactorily characterized by elemental analyses, IR and ^1H NMR [1].

*$[(MoO_2L^1)_2(4,4'\text{-azpy})].CHCl_3$ (**1**).* A mixture of 0.884 g (2 mmol) of MoO_2L^1 and 0.184 g (1mmol) of 4,4'-azopyridine in $CHCl_3$ (20 mL) was refluxed for 3 h. The solution was filtered. Shiny orange-red single crystals suitable for X-ray diffraction analysis were obtained after one day. Yield ~70%. Anal. Calc. for $C_{44}H_{38}S_4N_8O_6Cl_6Mo_2$ (%): C, 40.37; H, 2.90; N, 8.56; Mo, 14.68, Found: C, 40.28; H, 2.66; N, 8.60; Mo, 14.92, IR (KBr Pellet), cm^{-1}: $\nu_{(C=N)}$ 1596 (vs), $\nu_{(N=N)}$ 1533(s), $\nu_{[Mo\text{-}N(azo)]}$ 1230 (s), $\nu_{(Mo=O)}$ 931(vs), 902(s), $\nu_{(Mo\text{-}N)}$ 642(s), $\nu_{(Mo\text{-}S)}$ 436(m); UV-

Vis (CH_2Cl_2) [λ_{max} /nm (ε/$dm^3mol^{-1}cm^{-1}$)]: 292 (9830), 380 (3030); ^1H NMR($CDCl_3$): (H_3C-C=N) 2.93 s (6H), (-S-CH_2-Ph) 4.40 s (4H), (aromatic protons) 7.13-7.91 m (26H).

Complex **2** was prepared similarly by refluxing the corresponding parent MoO_2L complex with 4, 4′-azopyridine in a 2:1 molar ratio in $CHCl_3$ for 3 h. (Scheme 2). The solution was filtered and a dark orange compound was obtained by evaporation of the filtrate at room temperature. The compound was recrystallized from ethanol. Shiny orange-red single crystals suitable for X-ray diffraction analysis were obtained after one day. Yield ~ 70-75 %.

*[(MoO_2L^2)$_2$(4,4'-azpy)].0.5 EtOH, 0.5 H_2O (**2**).* Anal. Calc. for $C_{31}H_{32}S_4N_8O_7Mo_2$ (%): C, 39.21 ; H, 3.37 ; N, 11.80; Mo, 20.24, Found: C, 38.95; H, 3.25; N, 11.18; Mo, 19.98, IR (KBr Pellet), cm^{-1}: $\nu_{(C=N)}$ 1593 (vs), $\nu_{(N=N)}$ 1535(s), $\nu_{[Mo\text{-}N(azo)]}$ 1231(s), $\nu_{(Mo=O)}$ 926(vs), 899(s), $\nu_{(Mo\text{-}N)}$ 640(s), $\nu_{(Mo\text{-}S)}$ 440(m); UV-Vis (CH_2Cl_2) [λ_{max} /nm (ε/$dm^3mol^{-1}cm^{-1}$)]: 298 (6480), 347 (3070); ^1H NMR($CDCl_3$): (-S-CH_3) 2.62 s (6H), (H_3C-C=N) 2.99 s (6H), (aromatic protons) 7.17-7.95 m (16H).

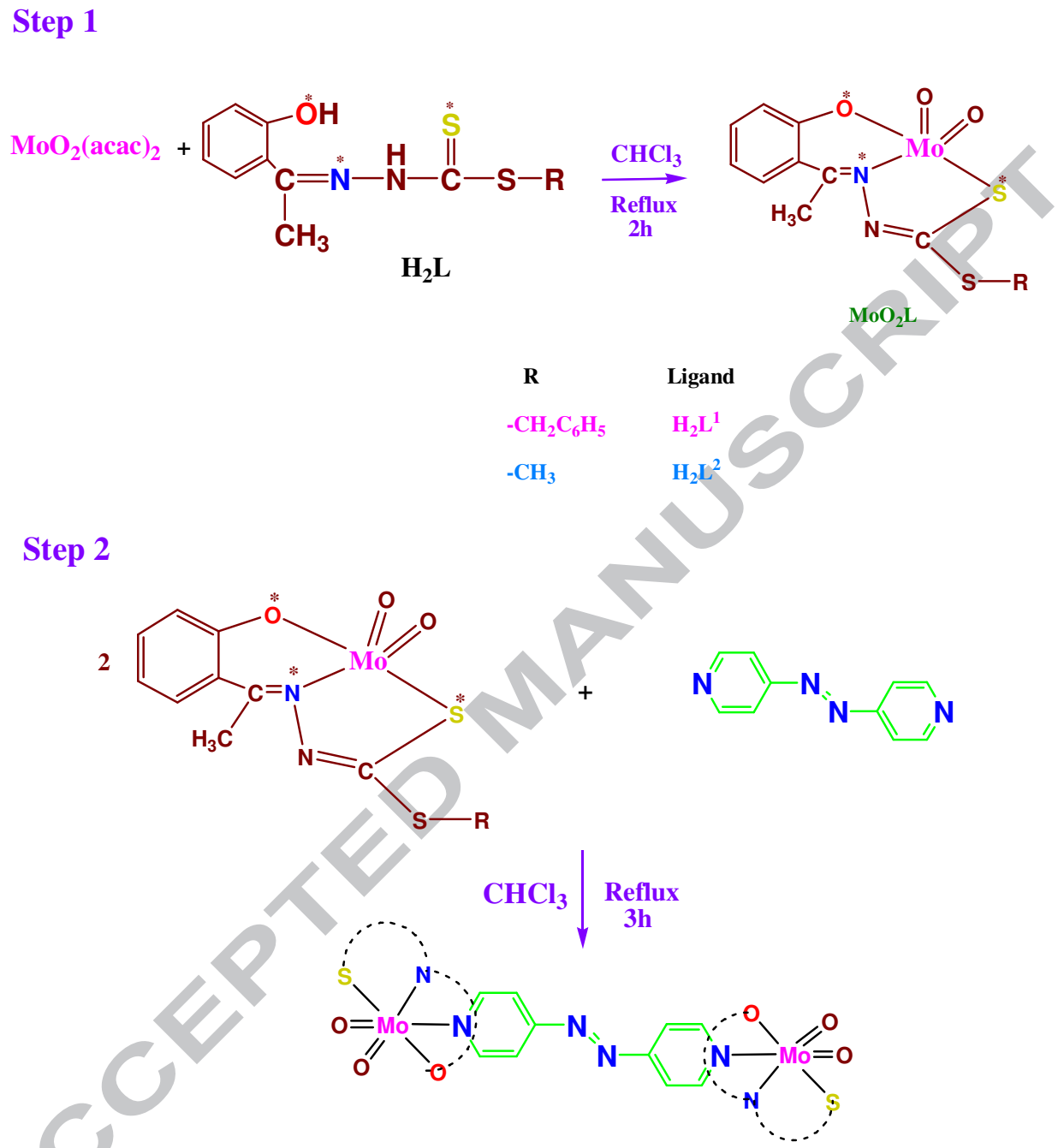

Scheme 2 Reaction diagram for the synthesis of $[(MoO_2L)_2(4,4'\text{-azpy})]$ complexes

2.3. Physical Measurements

Elemental analyses were performed on a Perkin-Elmer 240 C, H, N analyzer. Molybdenum was estimated gravimetrically by using oxine as the reagent following standard method. NMR spectra were recorded on a Bruker 300 L NMR spectrometer operating at 300 MHz with TMS as internal standard. IR spectra were recorded as KBr pellets on a Perkin-Elmer model 883 infrared spectrophotometer. Electronic spectra were recorded using a HITACHI U-3501 UV-Vis recording spectrophotometer. Magnetic susceptibility was measured with a PAR model 155 vibrating sample magnetometer with Hg $[Co(SCN)_4]$ as calibrant. Electrochemical data were collected on a Sycopel model AEW2 1820 F/S instrument at 298 K using a Pt working electrode, Pt auxiliary electrode and SCE reference electrode. Cyclic voltammograms were recorded in DMF containing 0.1 M TBAP (tetrabutylammonium perchlorate) as supporting electrolyte. Thermal analyses were carried out in a NETZSCH STA 449 *F3 Jupiter* thermal Analyzer in a dynamic atmosphere of dinitrogen (flow rate= 30 cm^3min^{-1}).

2.4. Crystallographic Measurements

The crystallographic data for complex **1** was collected on an Oxford Diffraction X-Calibur System and for **2** was collected on a Bruker APEX-II diffractometer with CCD-area detector. Both data sets were obtained with graphite-monochromated Mo-Kα (λ=0.71073Å) radiation. Unit-cell dimensions and intensity data for **1** and **2** were measured at 150(2) and 296(2) K respectively. Data analysis for **1** was carried out with the CrysAlis program [20] and for **2** with SAINT [21]. The crystal structures were solved by direct methods using SHELXS-97 [22] and refined by full-matrix least-squares based on F^2 with anisotropic displacement parameters of non-hydrogen atoms using SHELXL-97 [22]. The hydrogen atoms were included in calculated

positions. The structure of complex **2** contains superimposed solvent ethanol and water molecules both refined with 25% occupation. Absorption corrections for **1** were carried out with ABSPACK [23] and for **2** with SADABS [24]. The MERCURY [25] and DIAMOND [26] programs were used for presentation of the structures.

3. Computational details

The Gaussian 03 program [27] was used for all calculations. Starting models were taken from the crystal structures but with hydrogen atoms given theoretical positions. Methodology involved the B3LYP density functional together with basis sets LANL2DZ for Mo, 6-31+G* for S and 6-31G for the remaining atoms. Both single point calculations and geometry optimizations were carried out. Geometry optimized structures showed no negative frequencies and were therefore considered as true minima.

4. Results and discussion

4.1. Synthesis

The Schiff base ligands H_2L^1 and H_2L^2 were prepared by condensing 2-hydroxyacetophenone and S-benzyl/ S-methyl dithiocarbazate in ethanol. The ligands were satisfactorily characterized by elemental analyses, IR and ^{1}H NMR. Both the binuclear Mo(VI) complexes (**1**-**2**) of general formula $[(MoO_2L)_2(4,4'\text{-azpy})]$ were prepared by refluxing the corresponding parent MoO_2L complex with 4,4'-azpy in 2:1 molar ratios in chloroform.

The orange-red binuclear dioxomolybdenum(VI) complexes (**1-2**) are air stable in the solid state. The compounds are readily soluble in alcohol, CH_2Cl_2, CH_3CN, DMF and DMSO but are insoluble in water. The complexes are diamagnetic at room temperature as is expected for d^0 Mo(VI) centers [28]. Molar conductivity data in 10^{-3}M CH_2Cl_2 solution indicate that they are

non-electrolytes. All the binuclear Mo(VI) complexes are satisfactorily characterized by elemental analyses, IR, ^{1}H NMR, electronic spectra, cyclic voltammetry and thermogravimetric analysis. The complexes **1-2** have been structurally characterized by single crystal X-ray diffraction.

4.2. IR and ^{1}H NMR Spectra

Characteristic IR bands and assignments for the binuclear dioxomolybdenum(VI) complexes, $[(MoO_2L)_2(4,4'\text{-azpy})]$, are given in the experimental section. A strong $\nu_{(C=N)}$ band [29,30] was observed around 1593-1596 cm^{-1} region for the complexes. Bands at 640-642 cm^{-1} for the complexes are assigned to $\nu_{(Mo-N)}$ stretching [31]. The complexes exhibit a medium intensity band around 436-440 cm^{-1} assigned to $\nu_{(Mo-S)}$ stretching [32]. Like most *cis*-dioxomolybdenum(VI) complexes, two IR bands are observed in the 931-899 cm^{-1} region, the higher and lower frequency bands originating from the anti-symmetric and the symmetric stretching modes of the *cis*-$[MoO_2]^{2+}$ moiety [33-35]. It is revealed that the coordination of the neutral bidentate N-N donor ligand, 4,4′-azopyridine, has the effect of lowering the $\nu_{(Mo=O)}$ stretching frequencies [1]. The complexes exhibit strong bands around 1230-1231 cm^{-1} characteristic of $\nu_{[Mo-N(azo)]}$ stretching [36] which confirm the presence of coordinated 4,4′-azopyridine, as an ambidentate ligand. In the region expected for the N=N stretch vibration, complexes **1** and **2** exhibit one single, sharp and strong band at 1533 and 1535 cm^{-1} respectively attributable to the presence of the 4,4′-azopyridine moiety in the structures [37].

^{1}H NMR spectral data and their assignments for the ligands and complexes **1** and **2** in $CDCl_3$ are given in the experimental section. The signals in the spectra corresponding to N-H and O-H at δ 11.25, δ 11.26 ppm of H_2L^1 and at δ 11.42, δ 12.68 ppm of H_2L^2 disappear in **1** and **2** indicating

their deprotonation upon coordination of the ligand to molybdenum. In the complexes, the involvement of azomethine nitrogen is indicated by the shift of the $-CH_3$ proton signal from δ 2.47 to δ 2.93 ppm and δ 2.46 to δ 2.99 ppm respectively. This feature is indicative of a decrease in the electron density caused by the electron withdrawal by the molybdenum. The methylene protons of the ligand H_2L^1 at δ 4.41 ppm remain practically unaffected in **1** indicating the non-involvement of the S-benzyl sulphur in coordination. The methyl protons of the ligand H_2L^2 and complex **2** appear at nearly the same position. In complex **1**, 26 aromatic protons appear as multiplets within the range δ 7.13-7.91 ppm. Similar observation for aromatic protons is noted in case of H_2L^2 and its corresponding complex **2**.

Both the IR and ^{1}H NMR spectral data are in good agreement with the donor sites of the ligands that coordinate to the $[MoO_2]^{2+}$ centers. The ^{1}H NMR analysis also confirmed chemical structures for both the complexes in solution.

4.3. Electronic spectra

The electronic absorption spectra of the $[(MoO_2L)_2(4,4'\text{-azpy})]$ complexes **1** and **2** were recorded in dry CH_2Cl_2 and the spectral data are given in the experimental section. Both the complexes display a broad lowest energy absorption maximum in the 380-347 nm range which is assigned [38] to S(pπ)→Mo(dπ) LMCT transition involving the promotion of an electron from the filled HOMO of the ligand to the empty LUMO of molybdenum. The other LMCT bands in the 298-292 nm range [38-41] for both the complexes may be assigned to nitrogen to molybdenum and oxygen to molybdenum charge transfer transitions. The absence of a d-d transition absorption band in the visible region confirms the $4d^0$ electronic configuration of Mo(VI).

4.4. Electrochemical properties

The electron transfer behavior of the two binuclear [$(Mo^{VI}O_2L)_2$(4,4'-azpy)] complexes **1** and **2** have been studied by cyclic voltammetry. Cyclic voltammograms of the complexes at a Pt electrode were recorded in dry degassed DMF containing 0.1 (M) TBAP as the supporting electrolyte over a potential range of 0.00 to -1.50 V. Results of cyclic voltammetric studies of the complexes are presented in Table 1 and cyclic voltammograms are shown in Figures S1 and S2 The complexes **1** and **2** show two irreversible one electron two step reductions in the potential range -0.41 to -0.42 V and -0.82 to -0.85 V corresponding to Mo^{VI}-Mo^{VI} / Mo^{V}-Mo^{V} and Mo^{V}-Mo^{V} / Mo^{IV}-Mo^{IV} couples [42,43]. On scan reversal, two irreversible one electron two step oxidative responses are located in the potential range +0.43 to +0.46 V and +0.73 to +0.74 V which correspond to Mo^{IV}-Mo^{IV} / Mo^{V}-Mo^{V} and Mo^{V}-Mo^{V} / Mo^{VI}-Mo^{VI} couples. Thus, from the results it can be concluded that in aprotic solvent the reduction of these binuclear dioxomolybdenum complexes is generally irreversible.

Table 1

Cyclic voltammetric results[a] (V vs SCE) for the [$(Mo^{VI}O_2L)_2$(4,4'-azpy)] complexes at 298 K

Complexes	E_{pc} (V)	E_{pa} (V)
[$(MoO_2L^1)_2$(4,4′-azpy)] (**1**)	-0.41, -0.85	+0.43, +0.73
[$(MoO_2L^2)_2$(4,4′-azpy)] (**2**)	-0.42, -0.82	+0.46, +0.74

[a]*Solvent:* DMF (dry, degassed) ; supporting electrolyte: 0.1M TBAP ; solution strength: 10^{-3}M ; working electrode: platinum ; reference electrode: SCE; scan rate: 100 mVs^{-1}.

4.5. Thermogravimetric analysis and framework stability

Thermogravimetric analyses of complexes **1** and **2** were conducted in the temperature range 30-700˚C with a 10˚C/min interval in nitrogen atmosphere to assess their framework stabilities

(Figures S3 and S4). Above 175˚C, the TG/DTA curve exhibits three steps of weight loss. Complex **1** shows a weight loss of ~10% supported by an exothermic peak at 175˚C, which corresponds to the loss of one guest solvent $CHCl_3$ molecule (calc. 9.13%) and the framework is quite stable up to 350˚C. In the temperature range 350-370˚C, a ~35% weight loss was observed suggesting the concomitant loss of the second solvent $CHCl_3$ molecule and 4,4′-azpy spacer (calc. 32.33%). In the third step above 600˚C, a ~47.0% weight loss suggesting the removal of two molecules of $–CH_2Ph$ ligand fragments (calc. 46.25%). Upon further heating the compound decomposes to unidentified product. Similar decomposition profile was observed in case of complex **2**.

4.6. Oxo-transfer from Mo(VI) to substrate

Both the binuclear complexes **1** and **2** exhibit oxo-transfer reaction in dry degassed CH_3CN medium to the substrate PPh_3 forming the corresponding $Mo^{IV}OL$ complexes. The reaction may be represented as:

$$[(Mo^{VI}O_2L)_2(4,4'\text{-azpy})] + PPh_3 \xrightarrow{CH_3CN} 2\,Mo^{IV}OL + OPPh_3 + 4,4'\text{-azpy}$$

These complexes are non-electrolytes and diamagnetic in solid state at room temperature consistent with a d^2 Mo(IV) centre [43,44]. Like binuclear complexes **1** and **2**, the IR spectra of these Mo(IV) oxo complexes reveal that the main ligand framework with all its donor points remain unaltered. These complexes exhibit a single, sharp, strong band in the 970-965 cm^{-1} region, representing the $\upsilon_{(Mo=O)t}$ mode [45]. It is likely that $Mo^{IV}OL$ complexes are polymeric in nature via Mo=O···Mo linkages, a supposition which is supported by the presence of a medium intensity band around 815 cm^{-1} [46].

The electronic spectra in dry CH_2Cl_2 of the $Mo^{IV}OL$ complexes display several absorption bands in the 298-470 nm range including a new band in the low energy 470 nm region, which is a characteristic feature of the $[MoO]^{2+}$ core. A representative electronic spectrum is given in Fig. S5.

Electrochemical studies further support the formations of $Mo^{IV}OL$ complexes (Fig. S6). Both the complexes exhibit oxidation and reduction waves. An initial positive scan at a rate of 100 mV s^{-1} gives only a single irreversible oxidative response around +0.73 V, which is assigned to a Mo(IV)/Mo(VI) couple. On scan reversal, this Mo(VI) species exhibits two one-electron reductive responses around -0.45 V and -1.11 V corresponding to Mo(VI)/Mo(V) and Mo(V)/Mo(IV) processes [33], respectively. A representative cyclic voltammogram is shown in Fig. S6.

*4.7. Description of the crystal structures of complexes **1** and **2***

The orange-red binuclear complex **1** crystallized in the triclinic space group P-1 and complex **2** in the monoclinic space group C2/c. The molecular structure and atom numbering scheme of the complexes **1** and **2** are shown in Figures 1 and 2. Crystallographic data and refinement, selected bond lengths, bond angles and geometry of hydrogen bonding interactions are given in Tables 2-5, S1 and S2.

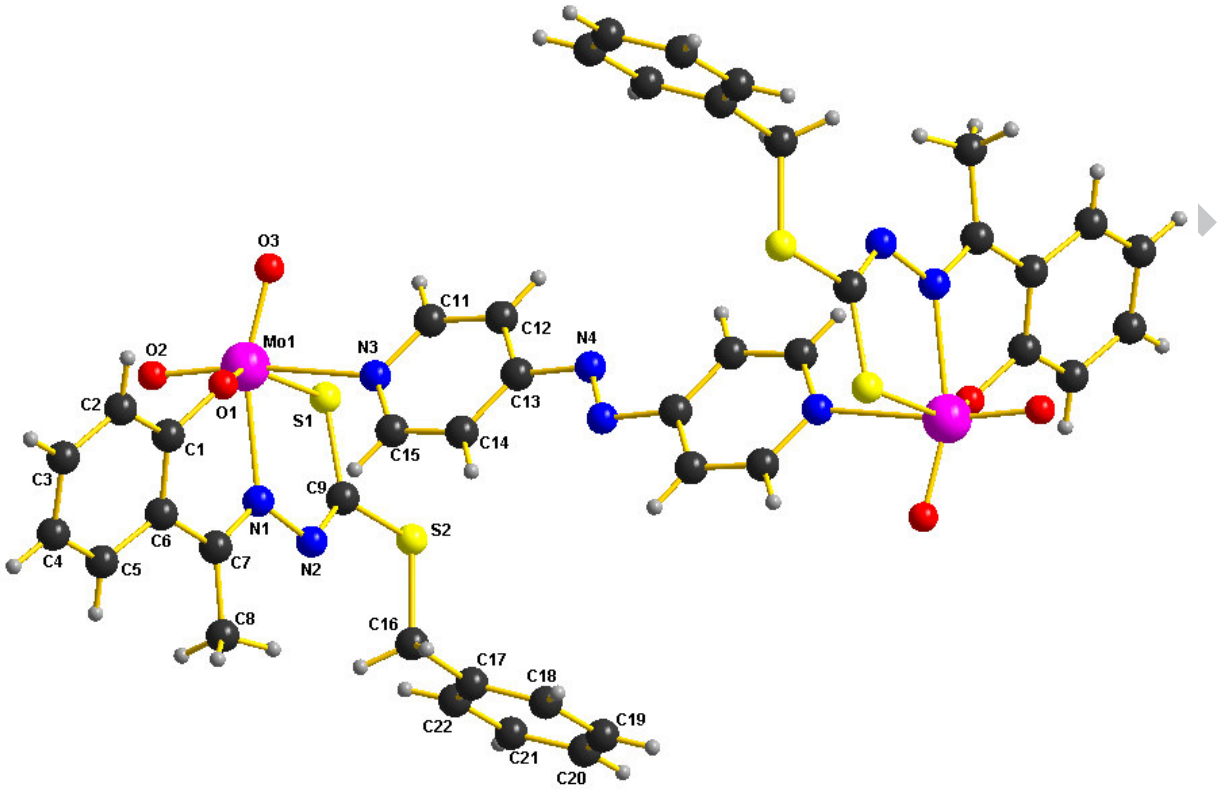

Fig. 1 Molecular structure of complex $[(MoO_2L^1)_2(4,4'\text{-azpy})]$ (**1**).

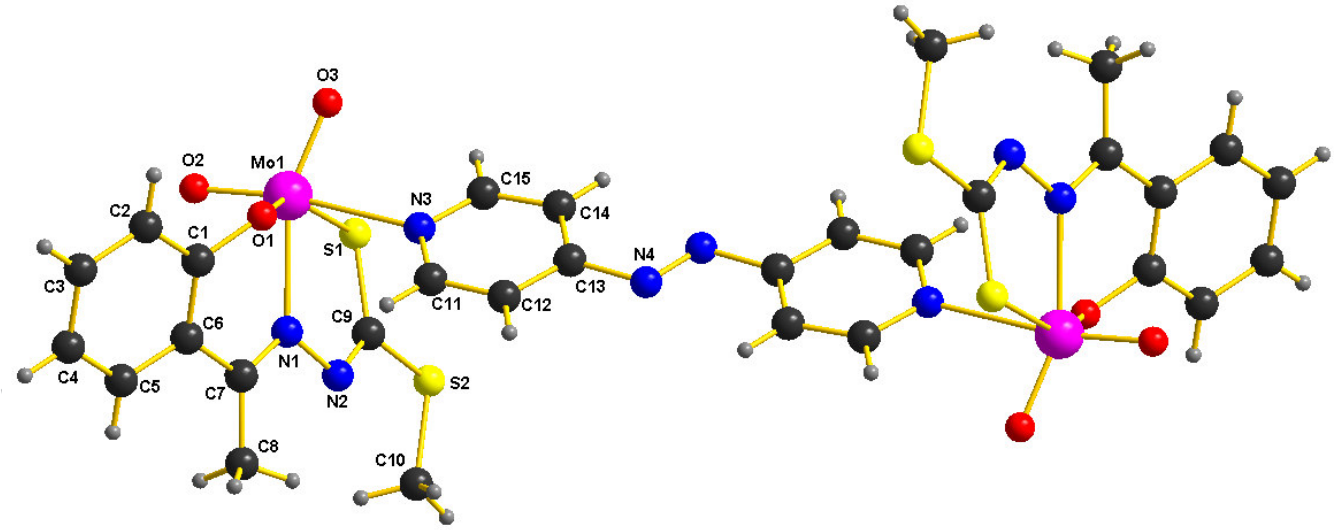

Fig. 2 Molecular structure of complex $[(MoO_2L^2)_2(4,4'\text{-azpy})]$ (**2**).

Table 2

Crystal data and details of refinement for complexes **1** and **2**

	Complex 1	**Complex 2**
Chemical formula	$C_{44}H_{38}S_4N_8O_6Cl_6Mo_2$	$C_{31}H_{32}S_4N_8O_7Mo_2$
Formula weight (M)	1307.64	948.77
Crystal system	triclinic	monoclinic
Space group	P-1	C2/c
a (Å)	7.5367(3)	38.22(3)
b (Å)	12.6164(5)	7.036(6)
c (Å)	14.6256(6)	17.466(14)
α(°)	96.928(3)	90.00
β (°)	100.339(3)	93.997(9)
γ(°)	104.358(4)	90.00
V (Å^3)	1305.33(10)	4685(7)
Z	1	4
Crystal size	0.13 x 0.03 x 0.03	0.20 x 0.18 x 0.16
Temperature (K)	150(2)	296(2)
D_C (g cm^{-3})	1.663	1.345
μ (Mo Kα) (mm^{-1})	1.002	0.759
F (000)	656	1912
Goodness of fit on F^2	1.011	1.074
R_1, wR_2 $[I > 2\sigma(1)]$	$R_1 = 0.0504$	$R_1 = 0.0447$
	$wR_2 = 0.1300$	$wR_2 = 0.1363$

$R = \sum ||F_o| - |F_c|| / \sum |F_o|$; $wR(F^2) = [\sum w(|F_o|^2 - |F_c|^2)^2 / \sum w |F_o|^4]^{1/2}$

Table 3

Experimental and calculated bond distances (Å) in **1** and **2**

	Complex 1		**Complex 2**	
Bond Distances(Å)	obs	calc	obs	calc
Mo(1)-O(2)	1.698(3)	1.737	1.688(3)	1.737
Mo(1)-O(3)	1.711(2)	1.746	1.705(3)	1.746
Mo(1)-O(1)	1.938(2)	1.971	1.934(3)	1.971
Mo(1)-N(1)	2.279(3)	2.340	2.287(4)	2.341
Mo(1)-S(1)	2.437(1)	2.474	2.446(2)	2.476
Mo(1)-N(3)	2.443(3)	2.503	2.461(4)	2.501

Table 4

Experimental and calculated bond angles (deg) in **1** and **2**

	Complex 1		**Complex 2**	
Bond Angles(deg)	obs	calc	obs	calc
O(2)-Mo(1)-O(3)	106.30(13)	106.20	106.02(17)	106.21
O(2)-Mo(1)-O(1)	98.28(13)	97.93	98.00(14)	97.89
O(3)-Mo(1)-O(1)	106.13(12)	108.46	107.26(16)	108.39
O(2)-Mo(1)-N(1)	90.89(12)	90.49	94.16(15)	90.49
O(3)-Mo(1)-N(1)	160.64(11)	160.54	157.53(13)	160.56
O(1)-Mo(1)-N(1)	79.44(10)	78.26	78.90(14)	78.30
O(2)-Mo(1)-S(1)	102.43(11)	101.68	98.69(12)	101.54
O(3)-Mo(1)-S(1)	90.75(9)	89.96	91.03(13)	90.03
O(1)-Mo(1)-S(1)	148.36(7)	148.07	150.66(10)	148.23
N(1)-Mo(1)-S(1)	76.60(7)	76.64	75.97(10)	76.65
O(2)-Mo(1)-N(3)	170.08(12)	171.72	171.21(14)	171.65
O(3)-Mo(1)-N(3)	83.21(11)	81.55	82.73(15)	81.65
O(1)-Mo(1)-N(3)	75.92(9)	76.48	78.32(13)	76.61
N(1)-Mo(1)-N(3)	80.20(9)	82.43	77.35(13)	82.29
S(1)-Mo(1)-N(3)	79.87(7)	80.93	81.61(10)	80.93
C(9)-S(1)-Mo(1)	98.90(11)	99.92	99.24(17)	99.81
C(1)-O(1)-Mo(1)	125.0(2)	128.28	121.9(3)	128.36
C(15)-N(3)-Mo(1)	122.0(2)	122.75	123.8(3)	122.73
C(11)-N(3)-Mo(1)	119.6(2)	118.11	119.3(3)	118.12
C(7)-N(1)-Mo(1)	124.3(2)	125.04	125.5(3)	124.97
N(2)-N(1)-Mo(1)	121.4(2)	120.15	120.7(3)	120.07

Table 5

Geometry of hydrogen-bonding interactions in the crystal structures of the complexes **1** and **2**

D-H	A	H···A (Å)	D···A (Å)	D-H···A (˚)	Symmetry code
*Complex **1***					
C(23)-H(23)	S(2)	3.14	3.998(6)	147	x, y, 1+z
C(16)-H(16A)	O(2)	2.50	3.438(5)	162	1-x, 1-y, 1-z
C(22)-H(22)	π^a	2.72	3.599	158	1-x, 1-y, 1-z
*Complex **2***					
C(5)-H(5)	O(2)	2.53	3.417(6)	160	½-x, ½-y, 1-z
C(8)-H(8C)	π^a	2.97	3.808	146	½-x, ½-y, 1-z

[a] centroid C(1)C(2)C(3)C(4)C(5)C(6)

Complexes **1** and **2** both contain crystallographic centres of inversion at the centre of the N=N bond of the 4,4′-azpy molecule. Analysis of bond lengths and angles revealed only small difference in the crystal structures of the complexes. The molybdenum atom exhibits a distorted octahedral coordination sphere comprised of two oxo-oxygen atoms O(2) and O(3), three donor atoms O(1), N(1), S(1) (phenolate oxygen, azomethine nitrogen and thioenolate sulphur) from the ligand and a nitrogen atom N(3) of the 4,4′-azpy molecule. Two asymmetric MoO_2L moieties are linked together via the 4,4′-azopyridine to form a binuclear dioxomolybdenum(VI) complex. The tridentate, dianionic ligand coordinated to the $[MoO_2]^{2+}$ core forming five and six membered chelate rings with bite angles of N(1)-Mo(1)-S(1), 76.60(6)˚, 75.97(10)˚ and N(1)-Mo(1)-N(3), 80.20(9)˚, 77.35(14)˚ respectively. Three donor atoms O(1), N(1), S(1) of the ligand and one terminal oxygen O(3) occupy the equatorial plane [38]. The oxo-oxygen O(2) and one terminal nitrogen N(3) of one half of the 4,4′-azpy occupy the axial position. The molybdenum(VI)

centres in the complexes **1** and **2** are displaced by 0.280 and 0.288 Å respectively from the mean plane N(3), S(1), O(1), O(2). In complexes **1** and **2** the non-bonding interatomic Mo···Mo separations are 13.863 and 13.881 Å respectively. The Mo(1)-N(3) bond lengths [2.443(3) and 2.462(4) Å] are longer than the other Mo(1)-N(1) bonds [2.279(3) and 2.287(4) Å] due to trans influence of O(2) which indicate the 4,4′-azpy nitrogen N(3) is comparatively weakly bonded to the $[MoO_2]^{2+}$ centre. The C(9)-S(1), C(9)-N(2) and N(1)-N(2) bond distances (Table 3) are comparable to those observed in similar binuclear dioxomolybdenum(VI) complexes [15b,16,47]. Intermolecular non-covalent interactions have been investigated to study the different crystal packing [48] and supramolecular framework formations. Both the Schiff base ligands provide potential supramolecular recognition sites for π···π stacking, C-H···π interaction and also act as hydrogen bond donors and acceptors to assemble supramolecular frameworks (Table 5).

As indicated in Fig. 3, complex **1** has C(16)-H(16A)···O(2) hydrogen bonding interactions operating between one of the oxo-oxygen O(2) (trans to 4,4′-azpy) of molybdenum and hydrogen atom of the S-benzyl moiety. The other oxo-oxygen O(3) does not participate in hydrogen bonding.

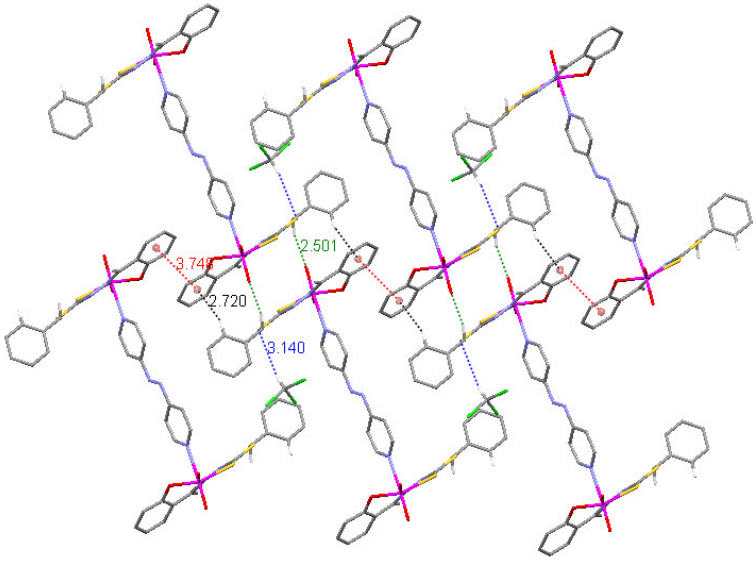

Fig. 3 Packing diagram of complex **1** showing various hydrogen bonding interactions H(23)···S(2) (blue dotted line), H(16A)···O(2) (green dotted line), H(22)··· π (black dotted line) and π···π stacking interaction (red dotted line), non-bonding hydrogen atoms are omitted for clarity.

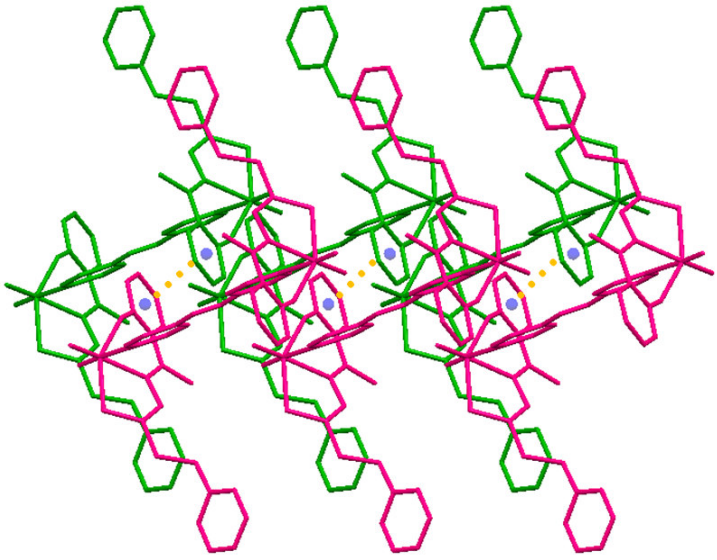

Fig. 4 Packing diagram of complex **1** along the c-axis. Stacking interactions of aromatic rings are shown as orange dotted lines between centroids in blue.

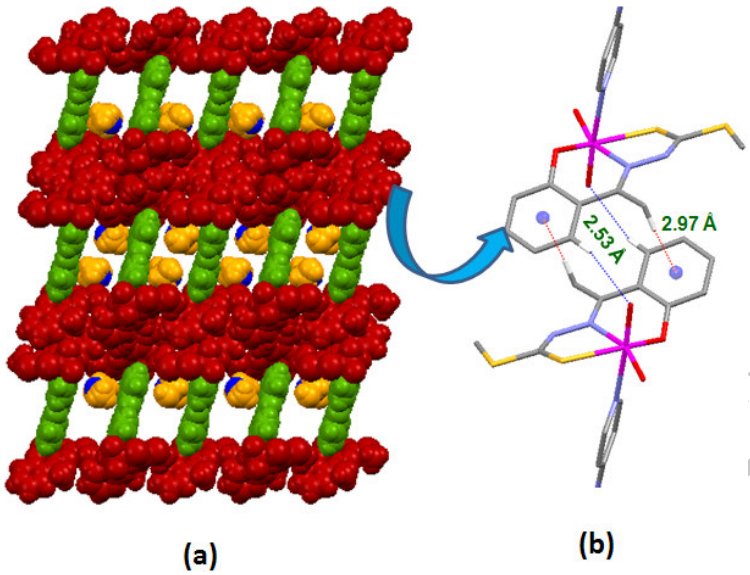

Fig. 5 (a) Formation of non-interpenetrated three-dimensional framework pillared by 4,4'-azopyridine spacer in complex **2**, the solvent molecules occupy the rectangular cavities; the azpy pillars are shown in green and the MoO_2L^2 layer is shown in red.

(b) Magnified view showing the hydrogen bonding interactions H(5)···O(2) (blue dotted line) and H(8C)···π (red dotted line), non-bonding hydrogen atoms are omitted for clarity.

In complex **1**, the π···π interaction [49] is another useful organizing force. The neighboring binuclear molecules are associated through face-to-face π···π stacking interactions (Fig. 4) with centroid-centroid distance 3.748 Å between the parallel aromatic phenyl rings of the acetophenone moiety thus, forming an interwoven 3D supramolecular network. The stability of the structure is further consolidated by the C-H···π interactions between the aromatic phenyl ring of the acetophenone moiety and H(22) of the phenyl ring of the S-benzyl moiety.

In complex **2** (Fig. 5b) also only one of the oxo-oxygens O(2) is involved in hydrogen bonding with H(5) of the acetophenone moiety. The C-H···π interactions help to extend the pillared

layers to a three dimensional architecture. Both the H(5)···O(2) and H(8C)···π hydrogen bonding interactions in complex **2** generate symbiotic donor-acceptor properties (Fig. 5b). In complex **2** although the adjacent layers of complexes are parallel, no π···π interaction is found because the layers direct at different orientations (Fig. 6).

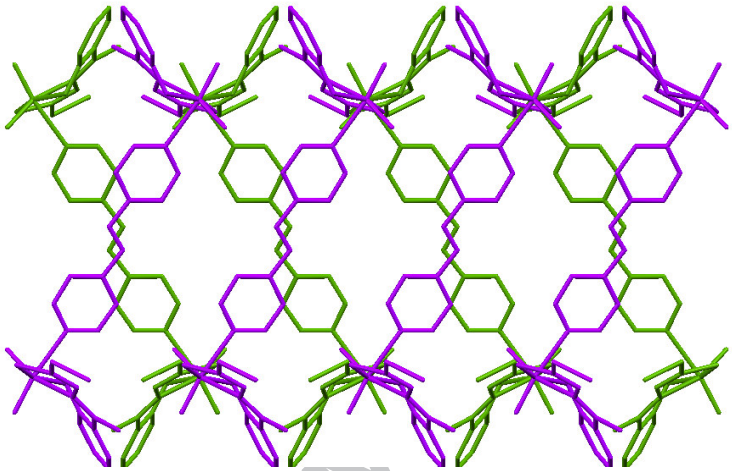

Fig. 6 Packing diagram of complex **2** along the c-axis.

The most intriguing structural feature of the supramolecular architectures is the formation of rectangular cavities. Since 4,4′-azpy (a rigid bridging ligand, of length ~8.99 Å) is employed as the organic spacer, each 3D supramolecular framework houses rectangular cavities [13.863 Å x 7.537 Å (**1**), 13.881 Å x 11.185 Å (**2**)] which facilitate the clathration of the solvent molecules. In complex **1**, the cavities host the solvent $CHCl_3$ molecules (Fig. 7) via H(23)···S(2) weak hydrogen bonding interactions. Here, the non-coordinated sulfur, S(2), of the S-benzyl moiety acts as the hydrogen bond acceptor [50].

It is interesting to note that despite the fact that $CHCl_3$ was used in the synthesis, it was not found in the cavities of **2**. Instead the cavity was occupied by a solvent ethanol molecule, used in the recrystallization and a water molecule, both refined with 25% occupancy (Fig. 5a).

The cavities are basically sustained by hydrogen bonding and aromatic-aromatic interactions, thus, giving rise to host-guest type of architectures.

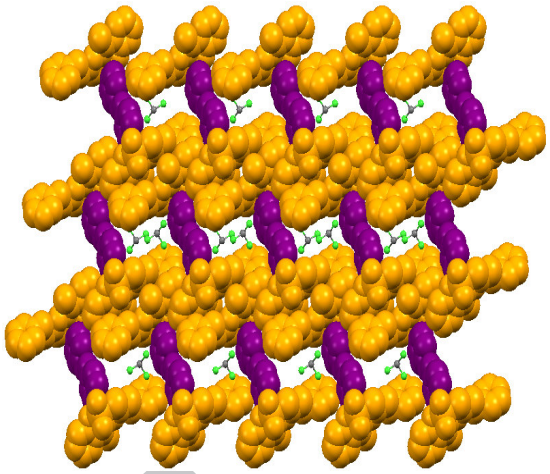

Fig. 7 Formation of non-interpenetrated three-dimensional framework pillared by 4,4'-azopyridine spacer in complex **1** along the a-axis, with solvent chloroform molecules occupying the rectangular cavities; the azpy pillars are shown in violet and the MoO_2L^1 layer is shown in yellow.

With subtle changes in the ligand substituent (i.e. S-benzyl/ S-methyl), supramolecular architectures having varied cavity size are formed. Compared to H_2L^2, H_2L^1 incorporates additional steric blockage due to the $–CH_2Ph$ bulky group, thereby leading to smaller sized cavities in complex **1** as compared to complex **2** (Fig. 8). Thus, the steric demands of the Schiff base ligands play a significant role in defining the cavity size of the crystalline frameworks.

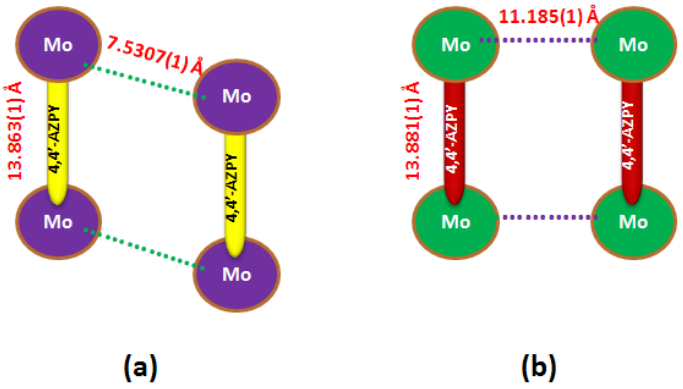

Fig. 8 Diagram illustrating the cavity formation in complex **1** (**a**) and complex **2** (**b**).

Similar binuclear dioxomolybdenum(VI) complexes with different spacers have been reported previously by our group [15b]. The spacers used therein [4,4'-bipyridine, 1,2-bis(4-pyridyl)ethene and 1,2-bis(4-pyridyl)ethane] did not give rise to pillared structures. Also cavity formation was observed only in one of the complexes. The cavity formation was very much different from those reported in the present work. Six binuclear moieties along with six floating methanol molecules together form a cylindrical cavity. The solvent molecules help in formation of cavities and are not entrapped in the cavities. On the other hand, in the presently reported compounds, only two binuclear moieties are capable of forming rhombus shaped cavities which entrap the solvent chloroform molecules. Hence, the use of 4,4'-azpy as a spacer in the present work gave rise to unique supramolecular frameworks.

*4.8. DFT calculations of complexes **1** and **2***

Both single point calculations and geometry optimizations of the complexes **1** and **2** have been carried out using DFT/ B3LYP methodology. The calculated bond distance and bond angles are given in Tables 3 and 4 and are in good agreement with the experimental data.

DFT calculations were also carried out to assess the importance of the intermolecular contacts listed in Table 5. In complex **1** a model was built consisting of one molecule of the complex together with two chloroform molecules attached via the C-H···S(2) interactions listed in Table 5. The energy of E(model) – E(complex)-2*E(chloroform) was -2.01 $kcalmol^{-1}$ showing only a very weak interaction. A second model was then built of the dimer (x, y, z; 1-x, 1-y, 1-z) which contains the two other interactions shown in Table 5. Now the energy of interaction E(dimer)-2*E(monomer) was -7.76 $kcalmol^{-1}$.

Both interactions shown for complex **2** in Table 5 involve molecules x, y, z and ½-x, ½-y, 1-z. The dimer shown in Fig. 4b was therefore built. The energy of interaction E(dimer)-2*E(monomer) was calculated as -10.42 $kcalmol^{-1}$

Analysis of the five HOMOs and LUMOs was also carried out for **1** and **2** after geometry optimization and show some notable features. The frontier orbitals are very similar in the two structures and therefore only those for **1** are reported here. Coefficients greater than 0.20 are noted in Table 6. There is no participation of the Mo atom orbitals in the five HOMOs. Instead the major contributions are only from N2, S1 and S2 and their symmetry equivalents. The coefficients for the LUMOs are very different. The two bridging nitrogen atoms N4, N4$1 of the bipyridine ligand play the major role in the LUMO which is of significant lower energy than the remaining four orbitals LUMO+1 to LUMO+4 for which the Mo orbitals play the largest role though with minor contributions from S1. LUMO+1, LUMO, HOMO, HOMO-1 are plotted in Fig. 9.

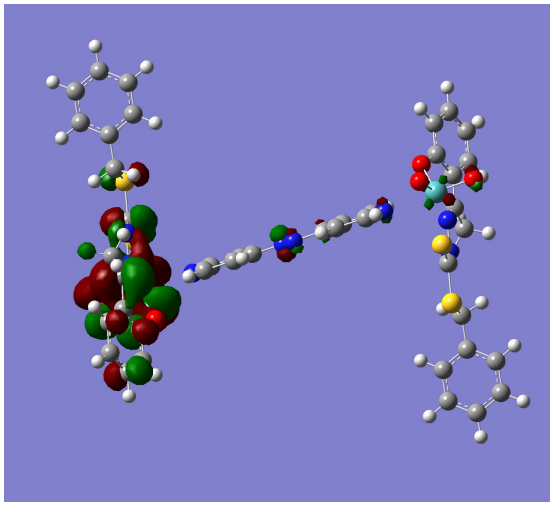

(a)

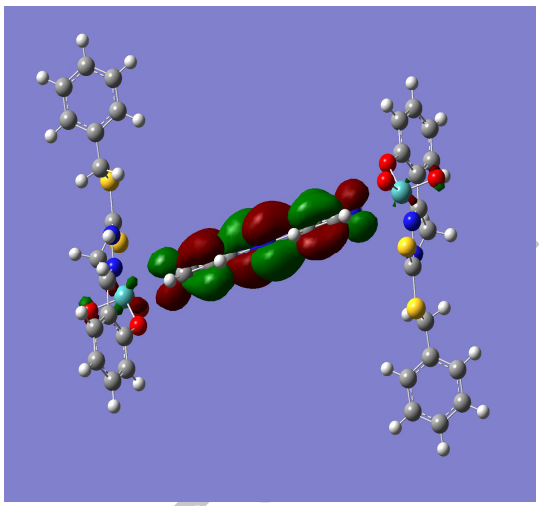

(b)

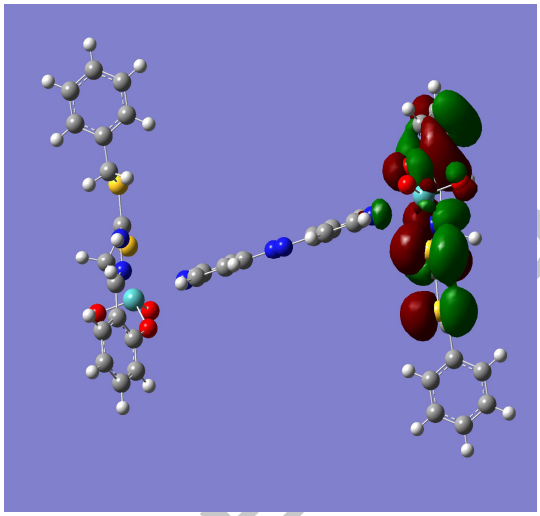

(c)

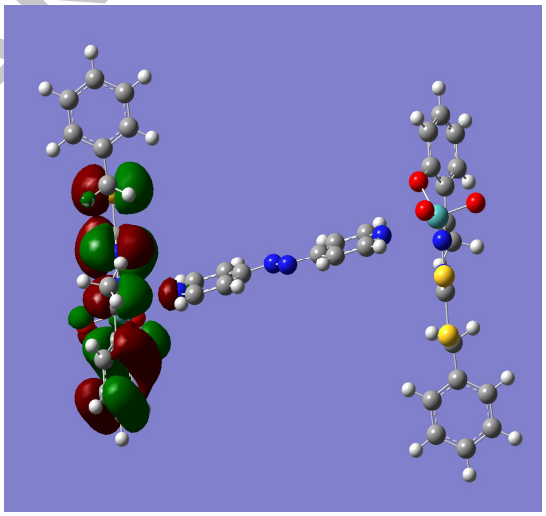

(d)

Fig. 9 Frontier orbitals in complex **1**, **(a)** LUMO+1 **(b)** LUMO **(c)** HOMO **(d)** HOMO-1

Table 6

Orbital contributions in complex **1**

Orbital	Eigen value	Major contributions (> 0.20) to the molecular orbitals
LUMO-4	-0.09075	Mo(1) $7d_0$ 0.525, $7d_{+1}$ 0.247, $7d_{-1}$ -0.270, $7d_{+2}$ 0.400, S1 $3p_y$ 0.208, $4p_y$ 0.234
LUMO -3	-0.09733	Mo(1)\$1 $7d_0$ 0.527, $7d_{+1}$ 0.248, $7d_{-1}$ -0.267, $7d_{+2}$ 0.395 S(1)\$1 $3p_y$ -0.208, $4p_y$ -0.232
LUMO -2	-0.09895	Mo(1) $7d_{+2}$ -0.306, $7d_{-2}$ 0.555
LUMO -1	-0.10607	Mo(1)\$1 $7d_{+2}$ -0.317, $7d_{-2}$ 0.564
LUMO	-0.13370	N(4) $2p_y$ 0.314, $3p_y$ 0.283, N(4)\$1 $2p_x$ -0.308, $3p_x$ -0.278
HOMO	-0.22503	N(2) $2p_x$ 0.281, S(1) $3p_x$ -0.272, S(2)\$1 $3p_x$-0.267
HOMO -1	-0.23051	N(2)\$1 $2p_x$ 0.282, S(2) $3p_x$ -0.267, S(1)\$1 $3p_x$-0.272
HOMO -2	-0.24193	S(1) $3p_x$ 0.490, $4p_x$ 0.270 S(2)\$1 $3p_x$ -0.358, $4p_x$ -0.200
HOMO -3	-0.24358	S(2)\$1 $3p_x$ 0.340 $4p_x$ 0.202
HOMO -4	-0.24733	S(2) $3p_x$ -0.405 $4p_x$ -0.228 S(1)\$1 $3p_x$ 0.497 $4p_x$ 0.274

\$1represents symmetry element 1-x, -y, -z

5. Conclusions

Two new 3D pillared binuclear dioxomolybdenum(VI) complexes **1** and **2** have been synthesized by using ONS donor ligands and 4,4′-azopyridine as a linker. Both the complexes were characterized by single crystal X-ray crystallography and various physicochemical techniques. Crystal structures reveal that in each of the complexes, the centrosymmetric structures consist of two MoO_2L moieties bridged by the two pyridine nitrogens of 4,4′-azpy which completes a distorted octahedral geometry. The azo (N=N) moiety does not contribute to the coordination properties of this ligand and no N=N bond cleavage takes place. TGA analysis proves well the framework stability of the two complexes. The electron transfer behavior shows that reduction of

the complexes in aprotic solvent is generally irreversible. In this work, the use of mixed ligands provides the possibility of generating multiple binding forces, such as coordination bonds, hydrogen bonding and other supramolecular interactions. This study clearly shows that in crystal structure of complex **1**, there is a strong tendency to form $\pi\cdots\pi$ stacking synthon between adjacent aromatic rings whereas no such interaction is found in complex **2**. By closely controlling the steric demands of the Schiff base, a remarkable class of supramolecular architectures containing diverse cavity size is formed. The cavities are capable of hosting guest solvent molecules. These results highlight the complexities of the self-assembly process and the need to understand the relative importance of the interactions between the molybdenum centers and ligands, as well as the solvent used during the crystallization process. The DFT calculations provide an energetic study of the non-covalent interactions in the complexes which are responsible for the supramolecular assemblies in the solid state. The calculations were also used to identify the compositions along with the energies of the relevant HOMOs and LUMOs.

Acknowledgements

D. Biswal acknowledges UGC, New Delhi for the Senior Research Fellowship. The authors thank the University of Reading and the EPSRC (U.K) for funds for the Oxford Diffraction diffractometer and Dr. Pramit Chowdhury (IIT Delhi) for the thermal analysis. We also thank Prof. Sudhanshu Sekhar Mandal and Dr. Tapas Kumar Raychaudhuri for fruitful discussions.

Appendix A. Supplementary data

Supplementary figures S1-S6 contain cyclic voltammograms, TG-DT curves, and electronic spectra of the complexes. CCDC 1416352 and 1416353 contains the supplementary crystallographic data for complexes **1** and **2** respectively. These data can be obtained free of

charge via http://www.ccdc.cam.ac.uk/conts/retrieving.html, or from the Cambridge Crystallographic Data Centre, 12 Union Road, Cambridge CB2 1EZ, UK; fax: (+44) 1223-336-033; or e-mail: deposit@ccdc.cam.ac.uk.

References

[1] N. R. Pramanik, S. Ghosh, T. K. Raychaudhuri, S. S. Chauduri, M. G. B. Drew, S. S. Mandal, J. Coord. Chem. 60 (2007) 2177–2190.

[2] M. R. Maurya, A. Kumar, A. R. Bahat, A. Azam, C. Bader, D. Rehder, Inorg. Chem. 45 (2006) 1260–1269.

[3] N. R. Pramanik, S. Ghosh, T. K. Raychaudhuri, S. Ray, R. J. Butcher, S. S. Mandal, Polyhedron 23 (2004) 1595–1603.

[4] M. Sutradhar, T. R. Barman, G. Mukherjee, M. G. B. Drew, Inorg. Chim. Acta 363 (2010) 3376–3383.

[5] M. Chakraborty, S. Roychowdhury, N. R. Pramanik, T. K. Raychaudhuri, T. K. Mondal, S. Kundu, M. G. B. Drew, S. Ghosh, S. S. Mandal, Polyhedron 50 (2013) 602– 611.

[6] M. B. Ferrari, F. Bisceglie, G. G. Fava, G. Pelosi, P. Tarasconi, R. Albertini, S. Pinelli, J. Inorg. Biochem. 89 (2002) 36–44.

[7] I. H. Hall, B. J. Barnes, J. E. Roswell, K. A. Shaffer, S. E. Cho, D. X. West, A. M. Stark, Pharmazie 56 (2001) 648–653.

[8] (a) J. R. Anacona, M. Rincones, Spectrochimica Acta A 141 (2015) 169-175; (b) E. N. Nfor, A. Husian, F. Majoumo-Mbe, I. N. Njah, O. E. Offiong, S. A. Bourne, Polyhedron 63 (2013) 207-213; (c) N. A. Mangalam, S. Sivakumar, M. R. Prathapachandra Kurup, E. Suresh, Spectrochimica Acta A 75 (2010) 686-692.

[9] (a) B. H. Northrop, D. Chercka, P. J. Stang, Tetrahedron 64 (2008) 11495−11503 (b) J.-P. Zhang, X.-C. Huang, Y.-M. Chen, Chem. Soc. Rev. 38 (2009) 2385−2396 (c) A. Y. Robin K. M. Fromm, Coord. Chem. Rev. 250 (2006) 2127−2157.

[10] L. Wang, Y. A. Li, F. Yang, Q. K. Liu, J. P. Ma, Y. B. Dong, Inorg. Chem. 53 (2014) 9087−9094.

[11] (a) A. M. Shultz, O. K. Farha, J. T. Hupp, S. T. Nguyen, J. Am. Chem. Soc. 131 (2009) 4204−4205 (b) M. H. Alkordi, Y. Liu, R. W. Larsen, J. F. Eubank, M. Eddaoudi, J. Am. Chem. Soc. 130 (2008) 12639−12641.

[12] L. Gao, C. Y. V. Li, K. Y. Chan, Z. N. Chen, J. Am. Chem. Soc. 136 (2014) 7209−7212.

[13] (a) S. Kitagawa, R. Matsuda, Coord. Chem. Rev. 251 (2007) 2490−2509 (b) M. Dinca, J. R. Long, Angew. Chem., Int. Ed. 47 (2008) 6766−6779.

[14] S. V. Kolotuchin, E. E. Fenlon, S. R.Wilson, C. J. Loweth, S. C. Zimmerman, Angew. Chem., Int. Ed. 34 (1995) 2654-2657.

[15] (a) D. Biswal, N. R. Pramanik, S. Chakrabarti, N. Chakraborty, K. Acharya, S. S.Mandal, S. Ghosh, M.G. B. Drew, T. K. Mondal, S. Biswas, New J. Chem. 39 (2015) 2778–2794. (b) N. R. Pramanik, M. Chakraborty, D. Biswal, S. S. Mandal, S. Ghosh, S. Chakrabarti, W. S. Sheldrick, M. G. B. Drew, T. K. Mondal, D. Sarkar, Polyhedron 85 (2015) 196–207. (c) W. Dong, C. Wang, Y. Ouyang, D. Z. Liao, Z. Anorg, Allg. Chem. 635 (2009) 544-548.

[16] D. Biswal, N. R. Pramanik, S. Chakrabarti, M. G. B. Drew, P. Mitra, K. Acharya, S. Biswas, T. K. Mondal, New J. Chem. 39 (2015) 8681-8694.

[17] J. W. Ko, K. S. Min, M. P. Suh, Inorg. Chem. 41 (2002) 2151-2157.

[18] (a) K. Fucke, N. Qureshi, D. S. Yufit, J. A. K. Howard, J. W. Steed, Cryst. Growth Des. 10 (2010) 880–886. (b) V. Vreshch, W. Shen, B. Nohra, S.-K. Yip, V. W.-W. Yam, C. Lescop, R. Reau,´ Chem. Eur. J. 18 (2012) 466–477.

[19] E. V. Brown, G. R. Granneman, J. Am. Chem. Soc. 97 (1975) 621–627.

[20] CrysAlis, Oxford Diffraction Ltd., Abingdon, U. K. (2006).

[21] SAINT, Bruker AXS Inc., Madison, Wisconsin, USA (2007).

[22] G. M. Sheldrick, Shelxs97 and Shelxl97, Programs for Crystallographic solution and refinement, Acta Cryst. A64 (2008) 112-122.

[23] ABSPACK, Oxford Diffraction Ltd., Oxford, U. K. (2005).

[24] G. M. Sheldrick, *SADABSs*, An empirical absorption correction program; Bruker AXS Inc., Madison, Wisconsin, USA (2001).

[25] C. F. Macrae, P. R. Edington, P. McCabe, E. Pidcock, G. P. Shields, R. Taylor, M. Towler, J. van de Streck, J. Appl. Cryst. 39 (2006) 453-457.

[26] K. Brandenburg, DIAMOND Crystal Impact GbR, Bonn, Germany (1999).

[27] M. J. Frisch, G. W. Trucks, H. B. Schlegel, G. E. Scuseria, M. A. Robb, J. R. Cheeseman, J. A. Montgomery, T. Vreven, K. N. Kudin, J. C. Burant, J. M. Millam, S. S. Iyengar, J. Tomasi, V. Barone, B. Mennucci, M. Cossi, G. Scalmani, N. Rega, G. A. Petersson, H. Nakatsuji, M. Hada, M. Ehara, K. Toyota, R. Fukuda, J. Hasegawa, M. Ishida, T. Nakajima, Y. Honda, O. Kitao, H. Nakai, M. Klene, X. Li, J. E. Knox, H. P. Hratchian, J. B. Cross, V. Bakken, C. Adamo, J. Jaramillo, R. Gomperts, R. E. Stratmann, O. Yazyev, A. J. Austin, R. Cammi, C. Pomelli, J .W. Ochterski, P. Y. Ayala, K. Morokuma, G. A. Voth, P. Salvador, J. J. Dannenberg, V. G. Zakrzewski, S. Dapprich, A. D. Daniels, M. C. Strain, O. Farkas, D. K. Malick, A. D. Rabuck, K.

Raghavachari, J. B. Foresman, J. V. Ortiz, Q. Cui, A. G. Baboul, S. Clifford, J. Cioslowski, B. B. Stefanov, G. Liu, A. Liashenko, P. Piskorz, I. Komaromi, R. L. Martin, D. J. Fox, T. Keith, M. A. Al-Laham, C. Y. Peng, A. Nanayakkara, M. Challacombe, P. M. W. Gill, B. Johnson, W. Chen, M. W. Wong, C. Gonzalez, J. A. Pople, Gaussian 03, revision C.02; Gaussian, Inc.: Wallingford . CT, U.S.A.

[28] E. I. Stiefel, Prog. Inorg. Chem. 22 (1977) 1.

[29] F. A. Cotton, R. M. Wing, Inorg. Chem. 4 (1965) 867-873.

[30] M. Goodgame, P. J. Hayward, J. Chem. Soc. A (1966) 632-634.

[31] Y.-L. Zhai, X.-X. Xu, X. Wang, Polyhedron 11 (1992) 415-418.

[32] M. Chaudhury, J. Chem. Soc. Dalton Trans. (1984) 115-120.

[33] C. Bustos, O. Burckhardt, R. Schrebler, D. Carrillo, A. M. Arif, A. H. Cowley, C. M. Numm, Inorg. Chem. 29 (1990) 3996-4001.

[34] R. H. Holm, P. Kennepohl, E. I. Solomon, Chem. Rev. (1996) 2239-2314.

[35] S. Bhattacharyya, S. B. Kumar, S. K. Dutta, E.R.T. Tiekink, M. Chaudhury, Inorg. Chem. 35 (1996) 1967-1973.

[36] K. Uzarevic, G. Pavlovic, M. Cindric, Polyhedron 52 (2013) 294-300.

[37] P. Kar, R. Biswas, M. G. B. Drew, A. Frontera, A. Ghosh, Inorg. Chem. 51 (2012) 1837-1851.

[38] M. Chaudhury, Inorg. Chem. 24 (1985) 3011-3017.

[39] R. Hahn, U. Kusthardt, W. Scherer, Inorg. Chim. Acta. 210 (1993) 177-182.

[40] R. Mattes, V. Mikloweit, Inorg. Chim. Acta. 122 (1986) L19-L20.

[41] A. P. Koley, S. Purohit, S. Ghosh, L.S. Prasad, P.T. Manoharan, J. Chem. Soc. Dalton Trans. (1988) 2607-2613.

[42] N. Gharah, S. Chakraborty, A. K. Mukherjee, R. Bhattacharyya, Chem. Commun. (2004) 2630-2632.

[43] S. Purohit, A. P. Koley, L. S. Prasad, P. T. Manoharan, S. Ghosh, Inorg. Chem. 28 (1989) 3735-3742.

[44] A. Rana, R. Dinda, P. Sengupta, S. Ghosh, L.R. Falvello, Polyhedron 21 (2002) 1023-1030, and references therein.

[45] N. R. Pramanik, S. Ghosh, T. K. Raychaudhuri, S. S. Mandal, J. Coord. Chem. 62 (2009) 3845–3852.

[46] I.W. Boyed, J.T. Spence, Inorg. Chem. 21 (1982) 1602-1606.

[47] N.R. Pramanik, S. Ghosh, T.K. Raychaudhuri, R.J. Butcher, S.S. Mandal, J. Coord. Chem. 64 (2011) 1207–1215.

[48] V. Vrdoljak, B. Prugovecki, D. M. Calogovic, T. Hrenar, R. Dreos, P. Siega, Cryst. Growth Des. 13 (2013) 3773-3784.

[49] A. Dutta, A. D. Jana, S. Gangopadhyay, K. K. Das, J. Marek, R. Marek, J. Brus, M. Ali, Phys. Chem. Chem. Phys. 13 (2011) 15845-15853.

[50] S. Khullar, S. K. Mandal, Cryst. Growth Des. 14 (2014) 6433−6444.

New pillared dioxomolybdenum(VI) complexes with ONS donor ligands and 4,4′-azopyridine spacer: 3D metal-organic supramolecular architectures and DFT calculations

Debanjana Biswal[a], Nikhil Ranjan Pramanik[*b], Syamal Chakrabarti[*a], Michael G.B Drew[c]

[a]*Department of Chemistry, University College of Science, 92, Acharya Prafulla Chandra Road, Kolkata:700009, West Bengal, India.*

[b]*Department of Chemistry, Bidhannagar College, EB-2,Sector-1, Salt Lake, Kolkata: 700064, India.*

[c]*Department of Chemistry, The University of Reading, Whiteknights, Reading RG66AD, UK.*

Graphical abstract (Pictogram):

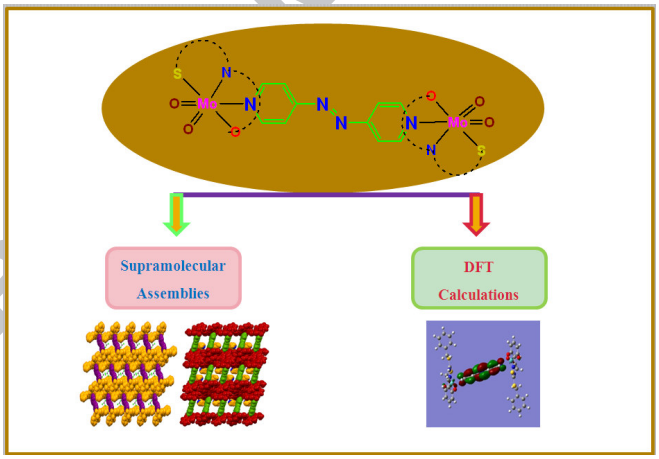

New pillared dioxomolybdenum(VI) complexes with ONS donor ligands and 4,4′-azopyridine spacer: 3D metal-organic supramolecular architectures and DFT calculations

Debanjana Biswal[a], Nikhil Ranjan Pramanik[*b], Syamal Chakrabarti[*a], Michael G.B Drew[c]

[a]*Department of Chemistry, University College of Science, 92, Acharya Prafulla Chandra Road, Kolkata:700009, West Bengal, India.*

[b]*Department of Chemistry, Bidhannagar College, EB-2,Sector-1, Salt Lake, Kolkata: 700064, India.*

[c]*Department of Chemistry, The University of Reading, Whiteknights, Reading RG66AD, UK.*

Graphical abstract (Synopsis):

By controlling the steric demands of the Schiff base, supramolecular architectures of Mo(VI) complexes containing diverse cavity sizes are formed.

New pillared dioxomolybdenum(VI) complexes with ONS donor ligands and 4,4′-azopyridine spacer: 3D metal-organic supramolecular architectures and DFT calculations

Debanjana Biswal[a], Nikhil Ranjan Pramanik[*b], Syamal Chakrabarti[*a], Michael G.B Drew[c]

[a]*Department of Chemistry, University College of Science, 92, Acharya Prafulla Chandra Road, Kolkata:700009, West Bengal, India.*

[b]*Department of Chemistry, Bidhannagar College, EB-2,Sector-1, Salt Lake, Kolkata: 700064, India.*

[c]*Department of Chemistry, The University of Reading, Whiteknights, Reading RG66AD, UK.*

HIGHLIGHTS:

- Synthesis of two new pillared binuclear dioxomolybdenum(VI) complexes with ONS donor ligands and 4,4′-azopyridine as a spacer.
- Spectral, electrochemical, thermal and structural characterizations of the synthesized complexes.
- 3D metal-organic supramolecular frameworks have rectangular cavities formed via hydrogen bonding and π-π stacking interactions.
- The DFT calculations provide an energetic study of the non-covalent interactions in the complexes.